PCCP

Accepted Manuscript

ROYAL SOCIETY OF CHEMISTRY

www.rsc.org/pccp

Cobalt Porphyrin Electrode Films for Electrocatalytic Water Oxidation

Ali Han,[a] Hongxing Jia,[a] Hao Ma,[a] Shifan Ye,[a] Haotian Wu,[a] Haitao Lei,[b] Yongzhen Han,[b] Rui Cao,*[b] and Pingwu Du*[a]

[a] CAS Key Laboratory of Materials for Energy Conversion, Department of Materials Science and Engineering, Department of Chemistry, University of Science and Technology of China (USTC), Hefei, China 230026. [b] Department of Chemistry, Renmin University of China, Beijing, China 100872

*Corresponding author: dupingwu@ustc.edu.cn, ruicao@ruc.edu.cn

Abstract: Catalysts play very important roles in artificial photosynthesis for solar energy conversion. In this present study, two water-insoluble cobalt porphyrin complexes, cobalt(II) *meso*-tetraphenylporphyrin (**CoP-1**) and cobalt(II) 5,10,15,20-tetrakis-(4-bromophenyl)porphyrin (**CoP-2**), were synthesized and coated as thin films on the FTO working electrode. The films showed good activities for electrocatalytic water oxidation in aqueous solutions at pH 9.2. The Faradic efficiencies for both films approached to ~100%, measured by fluorescence-based oxygen sensor. The turnover frequencies were close to 0.50 s^{-1} and 0.40 s^{-1} for **CoP-1** and **CoP-2**, respectively, under an applied anodic potential of 1.3 V (vs. Ag/AgCl) at pH 9.2. Importantly, no cobalt oxide particles were observed on the working electrode after catalysis. The stability of the catalyst films was further evaluated by UV-vis spectroscopy, inhibition measurement, mass spectrometry, scanning electron microscope (SEM) and energy dispersive X-ray spectroscopy (EDX). The pH dependence of water oxidation with **CoP-1** and **CoP-2** suggested a proton-coupled electron transfer (PCET) mechanism. The catalyst films could be recycled and showed almost unchanged catalytic activities when they were reused in new electrocatalytic studies for water oxidation.

1. Introduction

Due to the depletion of fossil fuels and many serious environmental problems accompanying their combustion,[1,2] it is highly urgent to seek new alternative energy resources. Hydrogen has received considerable attention as an ideal energy carrier because it is clean, renewable, cheap and carbon-neutral.[3] In the past three decades, major efforts have been devoted to discover reliable methods for hydrogen production *via* water splitting catalyzed by different kinds of homogeneous and heterogeneous systems.[4,5] Water splitting could be divided into two half-reactions: water reduction and water oxidation, and the latter reaction can provide both electrons and protons for the generation of hydrogen. In addition, the oxidation of water to oxygen (O_2) is a $4e^-/4H^+$ process and requires a high potential to realize the O-O bond formation, which has been proven to be particularly challenging.[6] Therefore, suitable water oxidation catalysts (WOCs) are demanding for this process.[7-9]

In nature, the oxidation of water is achieved at a $CaMn_4O_X$ active site of the oxygen evolving complex in Photosystem II (PSII) with quite high turnover frequencies (TOFs) of 100-400 s^{-1}.[10,11] To mimic the function of PSII, many metal oxide catalysts that promote the efficient splitting of water, such as ruthenium oxide,[12] iridium oxide,[13,14] cobalt oxide[5,15,16] and nickel oxide,[17] have been discovered. Meanwhile, attention has also been paid to molecular catalysts because they are more amenable for mechanistic studies by various spectroscopic, crystallographic and computational methods. Great progress has been made in water oxidation catalysis with different molecular transition metal complexes, including mononuclear,

binuclear and multinuclear complexes of ruthenium and iridium. Ruthenium-based molecular WOCs have been known since the early 1980s, including the famous ruthenium blue dimer, *cis,cis*-$[(bpy)_2(H_2O)RuORu(OH_2)(bpy)_2]^{4+}$.[18,19] It was recently found that a single Ru site, such as, $[Ru(tpy)(bpm)(OH_2)]^{2+}$ and $[Ru(tpy)(bpz)(OH_2)]^{2+}$ (bpm = 2,2′-bipyrimidine; bpz = 2,2′-bipyrazine), could also catalyze water oxidation as efficiently as multinuclear ones in aqueous solutions.[20] The Sun group reported a mononuclear Ru complex with a TOF of 300 s^{-1}, a value matching those found in nature.[21] As for iridium based WOCs, after the initial report of a binuclear iridium complex by the Bernhard group,[22] a series of mononuclear and binuclear Ir based molecular catalysts have been reported.[23-25] Due to the low abundance and high cost, limitations may arise from the use of catalysts containing these noble metals. More recently, efforts have been conducted to identify efficient first-row transition metal WOCs, such as manganese,[26-28] cobalt,[7,15,29] copper,[30-32] and iron.[33,34] In particular, cobalt based molecular WOCs, including cobalt polyoxometalate complexes,[35,36] Co_4O_4 cubane $[Co_4O_4(OAc)_4(py)_4]$,[37] mononuclear $[Co(PY5)(OH_2)](ClO_4)_2$ (PY5 = 6-(bis(bis-2-pyridyl)-methoxymethane)pyridine)[38] and cobalt(III) hangman corroles,[39,40] have received considerable attention due to their great activity and stability for water oxidation.

Molecular cobalt porphyrin complexes have been widely investigated as catalysts for hydrogen evolution.[41-43] Only a few examples in the literature reported the use of cobalt porphyrins as WOCs for oxygen evolution.[44,45] One early example used water-soluble cobalt meso-tetrakis(4-sulfophenyl)porphyrin as the catalyst and

$Ru(bpy)_3^{3+}$ as the oxidant for chemical water oxidation, giving an optimal O_2 yield of 65% calculated based on the oxidant. Recently, the Sakai group reported a similar system but took $Ru(bpy)_3^{2+}$ as a chromophore, $Na_2S_2O_8$ as a sacrificial electron acceptor and water-soluble cobalt porphyrin complexes as the catalysts for photocatalytic water oxidation. The highest turnover frequency (TOF) of 0.17 s^{-1} has been achieved and kinetic study showed that the oxygen evolution mechanism might involve either a radical coupling of two Co-oxyl radicals or disproportionation of two Co(IV) species. Meanwhile, the Groves group studied the electrocatalytic water oxidation using a varity of water-soluble cobalt porphyrin complexes.[45] Similarly, macrocyclic cobalt phthalocyanine was also previously reported as the WOC for oxygen evolution, either in aqueous solution for chemical water oxidation or on the electrode to form photoelectrode for photocatalysis.[46,47] It has been reported to immobilize catalysts on the surfaces of electrodes to construct water splitting devices without losing their reactivity and stability for the potential applications.[15,48] Based on this point, water-insoluble cobalt porphyrin complexes could allow facile fabrication of heterogeneous catalyst films on the electrode. Similar approach has recently been reported using cobalt polyoxometalates as catalysts for water oxidation.[49] On the other hand, like typical heterogeneous systems, water-insoluble catalysts could allow for easier post-reaction separation and recyclability. In some cases, they also give an enhanced catalytic stability. In this present paper, we reported two water-insoluble cobalt porphyrin complexes, cobalt(II) *meso*-tetraphenylporphyrin (**CoP-1**) and cobalt(II) 5,10,15,20-tetrakis-(4-bromophenyl)porphyrin (**CoP-2**) (scheme 1), to make

heterogeneous films on electrode for electrocatalytic water oxidation.

2. Experimental section

2.1 Materials

Cobalt acetate tetrahydrate ($Co(OAc)_2{\cdot}4H_2O$), potassium hydroxide (KOH), boric acid (H_3BO_3), tetrabutylammonium hexafluorophosphate, benzaldehyde, propionic acid, pyrrole, anhydrous tetrahydrofuran (THF), anhydrous dimethyl formamide, *p*-bromobenzaldehyde, nitrobenzene, acetic acid, methanol, chloroform were commercially available (from Aldrich or Acros company) and used without further purification. All electrolyte solutions were prepared with deionized water (Blue water Industry, resistivity: 18 MΩ·cm). The borate buffered solutions were prepared with H_3BO_3 and the pH was adjusted to 9.2 by KOH. Fluorine doped indium tin oxide (FTO) glass was purchased from Zhuhai Kaivo Electronic Components Co., Ltd. All experiments used FTO with 8-12 Ω /sq surface resistivity.

2.2 Synthesis

Synthesis of *meso*-tetraphenylporphyrin

A mixture of benzaldehyde (8.0 mL, 80 mmol) dissolved in propionic acid (300 mL) was heated up to 130 °C and was added with freshly distilled pyrrole (5.6 mL, 80 mmol). The mixture was stirred at 140 °C for 1 h and cooled to room temperature. The dark violet precipitate was collected by filtration and washed with methanol (50 mL × 3) to give *meso*-tetraphenylporphyrin as violet crystals (2.24 g) in a 18.2% yield. ^{1}H-NMR ($CDCl_3$, 300 MHz): δ (ppm) -2.76 (s, 2H, N-H), 7.76-7.78 (m, 12H, Ar-H), 8.23 (d, 8H, J = 8.8 Hz, Ar-H), 8.85 (s, 8H, pyrrole-H). UV-vis (λ) 416, 513, and 548

nm.

Synthesis of cobalt(II) *meso*-tetraphenylporphyrin (CoP-1)

To a solution of *meso*-tetraphenylporphyrin (232 mg, 0.25 mmol) in $CHCl_3$ (12 mL) and propionic acid (12 mL), was added $Co(OAc)_2{\cdot}4H_2O$ (622 mg, 2.50 mmol). After stirring this mixture at 120 °C for 1.5 h, the precipitate was filtered and washed with MeOH (10 mL × 3). The product was isolated by column chromatography as a brown solid (202 mg) in a 70% yield. Anal. Calcd. for $[Co(C_{44}H_{28}N_4)]$: C, 78.68; H, 4.20; N, 8.34. Found: C, 78.25; H, 3.99; N, 8.57. HRMS for $C_{44}H_{28}CoN_4$: calcd., 671.1646; found, 671.1897. UV-vis (λ): 415 and 531 nm.

Synthesis of 5,10,15,20-tetrakis-(4-bromophenyl)porphyrin

In a 500 ml round-bottom flask, nitrobenzene (100 ml), acetic acid (150 ml) and *p*-bromobenzaldehyde (3.72 g, 20 mmol) were mixed. After the solution was heated up to 125 °C, freshly distilled pyrrole (1.4 ml, 20 mmol) was rapidly injected into the system, and the mixture was stirred at 125 °C for 1 h. The solution was allowed to cool to room temperature and filtered. The dark purple precipitate was washed with methanol (50 mL × 3) to give product (1.42 g) in a 30.4% yield. ^{1}H-NMR ($CDCl_3$, 300 MHz): δ (ppm) -2.86 (s, 2H, N-H), 7.91 (d, 8H, J = 8.1 Hz, Ar-H), 8.08 (d, 8H, J = 8.4 Hz, Ar-H), 8.85 (s, 8H, pyrrole-H). UV-vis (λ): 419 and 513 nm.

Synthesis of cobalt(II) 5,10,15,20-tetrakis-(4-bromophenyl)porphyrin (CoP-2)

In a 100 ml round-bottom flask, $CHCl_3$ (25 ml), acetic acid (25 ml), $Co(OAc)_2{\cdot}4H_2O$ (1.2 g, 4.82 mmol) and 5,10,15,20-tetrakis-(4-bromophenyl)porphyrin (0.5 g, 0.538 mmol) were mixed. The mixture was refluxed at 120 °C for 1.5 h, and was then allowed to cool to room temperature and filtered. The brown precipitate was washed with methanol (50 mL ×

3) to give product (0.33 g) in a 62% yield. Anal. Calcd. for [Co($C_{44}H_{24}Br_4N_4$)]: C, 53.53; H, 2.45; N, 5.68. Found: C, 53.07; H, 2.29; N, 5.32. HRMS for $C_{44}H_{24}Br_4N_4Co$: calcd., 986.8026; found, 986.8423. UV-vis (λ): 417 and 543 nm.

2.3 Characterization.

^{1}H NMR and mass spectrometry. The ^{1}H NMR spectroscopic measurements were achieved on a Bruker spectrometer operating at 400 MHz (Bruker AV400). The data of high resolution mass spectrometry were acquired on a Bruker Daltonics Inc. LTQ Orbitrap XL hybrid Fourier Transform High-resolution Mass Spectrometer.

CoP Films Preparation. The as-synthesized cobalt porphyrin (CoP) complexes were used to make CoP electrode films on FTO glass plates for electrocatalysis. Prior to the test, FTO plates were cleaned by ultrasonication in deionized water, ethanol, acetone and deionized water for 5 minutes successively and dried in air. Then 1 mM stock solution of **CoP-1** or **CoP-2** was prepared using THF as the solvent. The catalysts were deposited onto FTO plates by drop casting to form thin catalyst films with 20 nmol/$cm^2_{geometric}$.

Cyclic Voltammetry. All electrochemical experiments were performed in a three-electrode system at room temperature with an electrochemical analyzer (660D CH Instrument, purchased from Shanghai Chenhua Instrument Co., Ltd.). FTO slides coated with molecular catalysts were used as working electrodes to obtain cyclic voltammograms. Ag/AgCl (3 M KCl) electrode was used as the reference electrode and the Pt wire was used as the counter electrode. The cyclic voltammograms were collected at 50 mV/s in a 0.5 M borate buffer solution (Bi, pH = 9.2). The CV scans

were recorded in a range of 0~1.5 V versus Ag/AgCl electrode (3 M KCl). There was an iR drop for compensation during the CV tests.

Faradaic efficiency. The quantitative detection of O_2 was realized by using fluorescence-based oxygen sensor (Ocean Optics). The test was carried out in a gas-tight electrochemical cell and the solution was degassed by bubbling with high purified N_2 for 0.5 h with stirring. The working electrodes were prepared by dropping the stock solution of **CoP-1** or **CoP-2** on FTO. The reference electrode was fixed at a position less than 1 cm from the surface of the catalyst films. Bulk electrolysis was carried out at 1.3 V in 0.5 M Bi solution for 2 h without iR drop compensation. The volume of the solution and the volume of the headspace in the working compartment were measured as 30 mL and 50 mL, respectively. The theoretical amount of O_2 was calculated by dividing the passed charge by 4F and the experimental amount of O_2 was calculated by converting the measured partial pressure of O_2 into mole numbers. The TOF was calculate by the following equation: TOF = the moles of the product/ the moles of the catalyst/time.

UV-vis spectroscopy. The UV-vis spectrophotometer (UNIC, 3802) was used to record the absorption spectra of the **CoP-1** and **CoP-2** solutions before and after electrolysis (dissolved by THF from FTO). The extinction coefficients of both cobalt complexes were measured in THF, which are 1.86×10^5 and 1.37×10^5 $M^{-1}\cdot cm^{-1}$, respectively. For the **CoP-1** and **CoP-2** solutions before electrolysis, the concentration is fixed at 1.67×10^{-6} M and their spectra were recorded. The FTO plates containing CoP films after electrolysis were initially washed by H_2O to remove the water-soluble

electrolyte and subsequently washed by 3 mL THF for 10 times (300 μL each), which were then used as the stock solution to make the sample at the concentration of 1.67×10^{-6} M for subsequent UV-vis measurements.

Recycling of CoP-1 samples on FTO electrode. After a certain time of electrolysis, the FTO plates containing **CoP-1** films were initially washed by H_2O to remove the water-soluble electrolyte and subsequently washed by 3 mL THF for 10 times (300 μL each), which were then concentrated to 30-50 μL under vacuum. The recycled concentrated **CoP-1** sample was reused for the preparation of electrode films by drop casting using a pipette. This process could be repeated to test the stability of the as-synthesized cobalt porphyrin complexes over the FTO conductive electrode.

Scanning electron microscope (SEM) and energy dispersive X-ray spectroscopy (EDX). The morphologies of the FTO surface before and after electrolysis were examined using a JSM-6700F field emission scanning electron microscope (FE-SEM). The EDX spectra were collected from three randomly selected areas of each sample. In addition, the materials were analyzed in several local spots to ensure their chemical homogeneity. The FTO electrodes were rinsed by THF and then coated with Au to make them conductive before loading into the instrument. Images were obtained with an acceleration voltage of 5 kV or 10 kV.

3. Results and discussion

Two cobalt porphyrin complexes (**CoP-1**/**CoP-2**) were synthesized using a modified method[50] and were well characterized. Cyclic voltammograms (CVs) of

CoP-1/**CoP-2** were first examined in a DMF solution (Figure S1). Both complexes showed no appreciable catalytic waves under 1.2 V (note: all the potentials in this paper are versus Ag/AgCl). Interestingly, addition of water to the DMF solutions produced obvious curves with an onset at 0.6 V for both **CoP-1** and **CoP-2**. The intensity of catalytic waves slightly increased when more water was added. These results prompted us to examine the electrochemistry of **CoP-1**/**CoP-2** in aqueous solutions. Since both complexes are water-insoluble, cobalt porphyrin based films were prepared by dropping 20 μL of the 1 mM stock solution onto the surface of FTO (1 cm^2) and then allowed to slowly evaporate in the air. The rough factor of FTO plates has been examined by CVs of ferro/ferricyanide couple versus $\nu^{1/2}$, which is ~ 1.11 (Figure S2). To simplify the calculation, the geometric area of FTO was directly used. The resulting films contained 20 nmol catalyst per cm^2 (geometric area) and the cobalt element was confirmed by energy dispersive X-ray diffraction (EDX) measurement (Figure S3). Subsequently, FTO glass slides coated with **CoP-1** or **CoP-2** film were used as the working electrode for electrocatalysis in a 0.5 M Bi solution. The cobalt based molecular catalysts and cobalt oxides are widely studied for water oxidation under near neutral pH (7-9).[16,39] We initially tried the as-prepared **CoP-1** film at pH = 7.59 and CoP-2 film at pH = 7.33 for water oxidation, but found their activities are quite low. However, at pH > 9.0, their catalytic activities could be significantly enhanced. Since we want to study water oxidation catalysis under benign conditions and the condition of pH > 10 is too harsh, pH 9.2 was therefore chosen as the main condition in this paper to study these CoP WOCs.

The CV results are shown in Figure 1. **CoP-1** has an obvious catalytic current after 1.00 V, which is about 0.53 V beyond the thermodynamic potential for water oxidation at pH = 9.2. This value is comparable to those recently reported for molecular cobalt catalysts.[36,39] Meanwhile, **CoP-2** displays an onset potential at 1.05 V, but the catalytic current increases at a much slower pace. During CV scans, gas bubbles on the surface of catalyst films could be clearly observed. In contrast, no appreciable catalytic current and gas bubbles could be observed in the range of 0-1.5 V using bare FTO plates as the working electrode under the same condition (Figure 1, black plot), indicating the important roles of **CoP-1** and **CoP-2** during water oxidation catalysis.

The Faradaic efficiencies of **CoP-1**/**CoP-2** were measured, as shown in Figure 2. The experiments of bulk electrolysis were carried out in an aqueous solution (0.5 M Bi, pH =9.2) in a sealed electrochemical cell under an atmosphere of N_2 at 1.3 V. O_2 was produced during the catalytic process in the presence of **CoP-1** or **CoP-2**, which was confirmed by gas chromatography (GC). The amount of O_2 in the headspace grew with the time of bulk electrolysis. To calculate the Faradaic efficiencies, all the currents were assumed for a $4e^-$ oxidation of water to produce O_2.[16] As seen from the data in Figure 2, **CoP-1** was more efficient than **CoP-2** as a WOC under the same condition. This observation is also consistent with the CV data, in which **CoP-1** had higher catalytic currents than **CoP-2** at applied potentials above 1.3 V. The TOFs were calculated to be 0.50 s^{-1} and 0.40 s^{-1} for **CoP-1** and **CoP-2**, respectively, at an overpotential of 820 mV. Figure 3a displayed the charges passed through electrodes

during water oxidation catalysis. More charges passed through **CoP-1** film than **CoP-2**. The black line in Figure 3a exhibited bulk electrolysis of the bare FTO as the working electrode, showing the passed charges were far less than the FTO decorated with **CoP-1/CoP-2** film. Figure 3b and 3c showed the photographs of O_2 bubbles on the working electrodes with **CoP-1** and **CoP-2** during water oxidation catalysis, indicating a catalytic O_2 evolution process. The current density for **CoP-1** could reach to ~3 mA/cm^2 in a 0.5 M Bi solution (Figure S4). The current densities are dependent on the ionic strength of the solutions. The value dropped to ~1.8 mA/cm^2 when bulk electrolysis was performed in a 0.1 M Bi solution.

No heterogeneous cobalt oxide materials were produced in the reaction systems when **CoP-1/CoP-2** were used water oxidation catalysis, as examined by different techniques, including UV-vis spectroscopy, mass spectrometry, inhibition experiment, SEM, and EDX measurements. All the results supported that these water-insoluble cobalt porphyrin complexes are molecular catalysts. First, the UV-vis spectra of **CoP-1** and **CoP-2** were measured under the same concentration before and after bulk electrolysis (Figure 4, the catalysts on FTO were washed out with THF). From Figure 4a, the used catalyst of **CoP-1** had almost the same absorption spectrum (red plot) as the freshly prepared **CoP-1** solution in THF (black plot) under the same concentration, maximized at 415 and 531 nm. The ratio of the intensity at two maximum peaks has slight difference, probably indicating the generation some reaction intermediate. It was the same case for **CoP-2**, showing nearly identical absorptions maximized at 417 and 543 nm before and after electrolysis (Figure 4b, black plot and red plot). No

appreciable changes of the absorption maximum peaks were observed based on their UV-vis spectra. Moreover, FTO plates washed by THF exhibited the same absorption properties with fresh FTO, as shown in Figure S5, indicating cobalt oxides were unlikely to deposit on FTO during bulk electrolysis.

Second, the **CoP-1/CoP-2** films after electrolysis were examined by mass spectrometry. After washing by THF, mass spectrometry showed that the exact molecular weight of **CoP-1/CoP-2** (m/z = 671.4443 for **CoP-1** and 986.7072 for **CoP-2**) existed in the washed solutions (Figure S6), suggesting the presence of the same substances of cobalt porphyrin complexes.

Third, scanning electron microscope (SEM) and transmission electron microscope (TEM) was used to examine the morphology of the working electrode (Figure 5 and Figure S7). The surface of the washed FTO after catalysis showed very similar features compared to the bare FTO. If there was partial decomposition of the cobalt complexes during the reaction, a clear morphology of particles would be observed on the FTO surface.[51] However, no such particles were detected in our SEM studies. After washing the used FTO electrodes with organic solvent, the "clean" FTO electrode was reused for bulk electrolysis, as shown in Figure S8. The "clean" FTO electrode had no significant difference from a pristine FTO electrode based on the data of the CV scans and the passed charges. The FTO electrode coated with a cobalt porphyrin complex showed obvious enhanced catalytic current. The electrolyte solution after electrolysis was further examined by TEM, as shown in Figure S9. The data show that no obvious nanoparticles are present in the solution. In addition, we

found some black spots in solution, but EDX data show these spots mainly contain K, O and Cu elements. K is probably from the solution for TEM measurement and Cu is from the copper grid.

Fourth, EDX data also revealed that only Sn, O and F elements existed on the washed electrode after catalysis. Sn element showed peaks at 3.44 keV and 3.65 keV, O gave the typical peak at 0.50 keV and F had the peak at 0.40 keV. These three elements could possibly come from FTO layer (Figure 5b and Figure S7c). Importantly, no other elements, especially cobalt, were found from EDX results.

Fifth, inhibition experiments were done to test if Co(II) ions were released into the solution. The ligand 2,2′-bipyridine (bpy) was used as the cobalt metal ion inhibitor during water oxidation catalysis. In a 0.5 M Bi solution containing 20 nmol Co^{2+} ions, addition of 80 μmol bpy as the Co^{2+} inhibitor could restrain the catalytic activity for water oxidation (Figure S10). In contrast, addition of the same amount of bpy to the solutions using **CoP-1/CoP-2** films for catalysis did not result in significant changes on their catalytic activities (Figure 6), suggesting that no Co^{2+} ions were found in the solutions. These observations also indicated that no Co^{2+} ions were released from **CoP-1/CoP-2** films during water oxidation catalysis.

The tafel plots of **CoP-1/CoP-2** were studied during the water oxidation reaction (Figure 7). The current densities were measured as a function of the overpotential (η). A slope of ~62 mV/decade was obtained for **CoP-1**, which is related to a chemical rate limiting step.[39] At pH 9.2, appreciable catalytic current is observed starting at η = 0.30 V for **CoP-1**. A similar slope of ~59 mV/decade was found for **CoP-2**.

To establish the proton and electron dependencies of water oxidation catalyzed by **CoP-1** and **CoP-2**, the pH dependence experiments were studied. The results showed that the overpotential decreased with the increase of pH values (Figure 8). After 1 h of electrolysis, the electrolytes were measured by inductive coupling plasma optical emission spectrometer (ICP-OES) at pH 4.7, 9.2 and 13. There were no remarkable Co element detected in all of the solutions. Therefore, similar stability was observed for operation under higher and lower pH conditions that are shown in Figure 8. To confirm this point, bulk electrolysis experiments were run with one single electrode for further examination under different pH conditions: pH=4.7 in an acetate solution, pH=9.2 in a borate solution, and pH=13.0 in a potassium hydroxide solution. All experiments were carried out at 1.3 V for 60 min, as shown in Figure S11. The results showed the passed charges increased with the operation time during the catalytic water oxidation reaction. The charges are proportional to the pH values and the operation time. The plot for pH 4.7 is quite low because the CV scans shown in Figure 8 indicate no obvious catalytic reaction could be observed at 1.3 V when pH < 5.0. Therefore, good stability was observed for electrolysis under high and low pH conditions. For a fixed catalytic current of **CoP-1** at 200 $\mu A/cm^2$, a plot of the potentials versus pH values showed a nearly linear decrease from pH = 13 to pH = 3 with a slope of -84 mV/pH unit (Figure 8b). As for **CoP-2**, the plot gave a similar slope of -88 mV/pH unit at 30 $\mu A/cm^2$ (Figure 8d). These values are higher than the theoretical value of -59 mV/pH unit, which was predicted by Nernst equation for a $1e^{-}$-$1H^{+}$ process. As a matter of fact, a slope of -90 mV/pH unit corresponds to the

loss of $1e^-$ accompanied by the transfer of ~1.5 protons. This suggests that a $2e^-$-$3H^+$ process may take place in the present systems, as have been previously reported for $CoH^{\beta F}CX$-COOH molecular WOC with an observed slope of -88 mV/pH unit.[39] A $2e^-$ electron transfer process has also been reported in many cobalt based catalysts for oxygen reduction reaction,[52] which is a reverse reaction to oxygen evolution from water. These results indicated a proton-coupled electron transfer (PCET) mechanism occurred during water oxidation reaction. In addition, decomposition of the cobalt complexes to cobalt oxide was unlikely because the latter species should be unstable in strong acid solutions during pH dependence experiments.

Compared to homogeneous systems, one advantage of heterogeneous catalysts lies in the easier post-reaction separation and recyclability. The present water-insoluble cobalt porphyrin complexes could modify the conductive electrode and catalyze water oxidation on the surface of the electrode in aqueous solutions, behaving like heterogeneous catalysts. Further evidences showed that these complexes held the molecular character and could be washed off the electrode by organic solvents. Therefore, it is important to examine the recyclability of the catalyst. Figure 9 shows five cycles of the electrocatalytic water oxidation activity for **CoP-1** after it was recycled and reused. Each cycle was performed for bulk electrolysis in a 0.5 M Bi buffered solution at pH 9.2 for one hour and reused for another cycle. The plots showed that **CoP-1** film had only slight decrease in their catalytic activities. To check the consistency on the use of different working electrode, bulk electrolysis experiments were further run with glass carbon electrode (Figure S12). The

performance of catalytic water oxidation showed similar stability as the experiment obtained using FTO electrode. All the results indicated that the present water-insoluble cobalt porphyrin complex displayed good recyclability for catalytic water oxidation for a few cycles.

Conclusion

In summary, we reported here cobalt porphyrin films coated on FTO as heterogeneous catalysts for water oxidation. Both **CoP-1** and **CoP-2** could catalyze water oxidation and the Faradaic efficiencies were close to ~100%. At an overpotential of 820 mV, the TOFs for **CoP-1** and **CoP-2** were 0.50 s^{-1} and 0.40 s^{-1}, respectively. More importantly, the complexes were stable under the catalytic conditions, as examined by UV-vis spectroscopy, mass spectrometry, inhibition experiments, SEM and EDX measurements. The pH dependence of the water oxidation reaction suggested a proton-coupled electron transfer (PCET) mechanism. Meanwhile, like typical heterogeneous catalysts, the present water-insoluble cobalt porphyrin complexes show good recyclability.

Acknowledgement

This work was financially supported by the National Natural Science Foundation of China (No. 21271166 to P.D. and No. 21101170 to R.C.), the Fundamental Research Funds for the Central Universities, Program for New Century Excellent Talents in University (NCET) and Young Thousand Talented Program.

References

(1) Gray, H. B. *Nature* **2009**, *1*, 7.
(2) Liu, X.; Du, P.; Cao, R. *Nat. Commun.* **2013**, *4:2375*, doi: 10.1038/ncomms3375.
(3) Lewis, N. S.; Nocera, D. G. *Proc. Natl. Acad. Sci. U.S.A.* **2006**, *103*, 15729-15735.
(4) Esswein, A. J.; Nocera, D. G. *Chem.Rev.* **2007**, *107*, 4022-4047.
(5) Kanan, M. W.; Surendranath, Y.; Nocera, D. G. *Chem. Soc. Rev.* **2009**, *38*, 109-114.
(6) Barber, J. *Chem. Soc. Rev.* **2009**, *38*, 185-196.
(7) Du, P.; Eisenberg, R. *Energy Environ. Sci.* **2012**, *5*, 6012-6021.
(8) Duan, L.; Tong, L.; Xu, Y.; Sun, L. *Energy Environ. Sci.* **2011**, *4*, 3296-3313.
(9) Cao, R.; Lai, W.; Du, P. *Energy Environ. Sci.* **2012**, *5*, 8134-8157.
(10) Barber, J. *Inorg. Chem.* **2008**, *47*, 1700-1710.
(11) Ferreira, K. N.; Iverson, T. M.; Maghlaoui, K.; Barber, J.; Iwata, S. *Science* **2003**, *303*, 1831-1838.
(12) Harriman, A.; Pickering, I. J.; Thomas, J. M.; Christensen, P. A. *J. Chem. Soc., Faraday Trans. I* **1988**, *84*, 2795-2806.
(13) Zhao, Y.; Hernandez-Pagan, E. A.; Vargas-Barbosa, N. M.; Dysart, J. L.; Mallouk, T. E. *J. Phys. Chem. Lett.* **2011**, *2*, 402-406.
(14) Morris, N. D.; Mallouk, T. E. *J. Am. Chem. Soc.* **2002**, *124*, 11114-11121.
(15) Nocera, D. G. *Acc. Chem. Res.* **2012**, *45*, 767-776.
(16) Kanan, M. W.; Nocera, D. G. *Science* **2008**, *321*, 1072-1075.
(17) Dincă, M.; Surendranath, Y.; Nocera, D. G. *Proc. Natl. Acad. Sci. U.S.A.* **2010**, *107*, 10337-10341.
(18) Gilbert, J. A.; Eggleston, D. S.; Murphy, W. R.; Geselowitz, D. A.; Gersten, S. W.; Hodgson, D. J.; Meyer, T. J. *J. Am. Chem. Soc.* **1985**, *107*, 3855-3864.
(19) Gersten, S. W.; Samuels, G. J.; Meyer, T. J. *J. Am. Chem. Soc.* **1982**, *104*, 4029-4030.
(20) Concepcion, J. J.; Jurss, J. W.; Brennaman, M. K.; Hoertz, P. G.; Patrocinio, A. O. v. T.; Iha, N. Y. M.; Templeton, J. L.; Meyer, T. J. *Acc. Chem. Res.* **2009**, *42*, 1954-1965.
(21) Duan, L.; Bozoglian, F.; Mandal, S.; Stewart, B.; Privalov, T.; Llobet, A.; Sun, L. *Nature Chem.* **2012**, *4*, 418-423.
(22) McDaniel, N. D.; Coughlin, F. J.; Tinker, L. L.; Bernhard, S. *J. Am. Chem. Soc.* **2008**, *130*, 210-217.
(23) Blakemore, J. D.; Schley, N. D.; Balcells, D.; Hull, J. F.; Olack, G. W.; Incarvito, C. D.; Eisenstein, O.; Brudvig, G. W.; Crabtree, R. H. *J. Am. Chem. Soc.* **2010**, *132*, 16017-16029.
(24) Lalrempuia, R.; McDaniel, N. D.; Muller-Bunz, H.; Bernhard, S.; Albrecht, M. *Angew. Chem. Int. Ed.* **2010**, *49*, 9765-9768.
(25) Cao, R.; Ma, H.; Geletii, Y. V.; Hardcastle, K. I.; Hill, C. L. *Inorg. Chem.* **2009**, *48*, 5596-5598.
(26) Dismukes, G. C.; Brimblecombe, R.; Felton, G. A. N.; Pryadun, R. S.; Sheats, J. E.; Spiccia, L.; Swiegers, G. F. *Acc. Chem. Res.* **2009**, *42*, 1935-1943.

(27) Brimblecombe, R.; Dismukes, C.; Swiegersc, G. F.; Spiccia, L. *Dalton Trans.* **2009**, 9374-9384.
(28) McEvoy, J. P.; Brudvig, G. W. *Chem. Rev.* **2006**, *106*, 4455-4483.
(29) Artero, V.; Chavarot-Kerlidou, M.; Fontecave, M. *Angew. Chem. Int. Ed.* **2011**, *50*, 7238-7266.
(30) Zhang, M.-T.; Chen, Z.; Kang, P.; Meyer, T. J. *J. Am. Chem. Soc.* **2013**, *135*, 2048-2051.
(31) Chen, Z.; Meyer, T. J. *Angew. Chem. Int. Ed.* **2013**, *52*, 700-703.
(32) Barnett, S. M.; Goldberg, K. I.; Mayer, J. M. *Nature Chem.* **2012**, *4*, 498-502.
(33) Fillol, J. L.; Codolà, Z.; Garcia-Bosch, I.; Gómez, L.; Pla, J. J.; Costas, M. *Nature Chem.* **2011**, *3*, 807-813.
(34) Ellis, W. C.; McDaniel, N. D.; Bernhard, S.; Collins, T. J. *J. Am. Chem. Soc.* **2010**, *132*, 10990-10991.
(35) Huang, Z.; Luo, Z.; Geletii, Y. V.; Vickers, J. W.; Yin, Q.; Wu, D.; Hou, Y.; Ding, Y.; Song, J.; Musaev, D. G.; Hill, C. L.; Lian, T. *J. Am. Chem. Soc.* **2011**, *133*, 2068-2071.
(36) Yin, Q.; Tan, J. M.; Besson, C.; Geletii, Y. V.; Musaev, D. G.; Kuznetsov, A. E.; Luo, Z.; Hardcastle, K. I.; Hill, C. L. *Science* **2010**, *328*, 342-345.
(37) McCool, N. S.; Robinson, D. M.; Sheats, J. E.; Dismukes, G. C. *J. Am. Chem. Soc.* **2011**, *133*, 11446-11449.
(38) Wasylenko, D. J.; Ganesamoorthy, C.; Borau-Garcia, J.; Berlinguette, C. P. *Chem. Commun.* **2011**, *47*, 4249-4251.
(39) Dogutan, D. K.; McGuire Jr., R.; Nocera, D. G. *J. Am. Chem. Soc.* **2011**, *133*, 9178-9180.
(40) Lai, W.; Cao, R.; Dong, G.; Shaik, S.; Yao, J.; Chen, H. *J. Phys. Chem. Lett.* **2012**, *3*, 2315-2319.
(41) Kellett, R. M.; Spiro, T. G. *Inorg. Chem.* **1985**, *24*, 2373-2377.
(42) Lee, C. H.; Dogutan, D. K.; Nocera, D. G. *J. Am. Chem. Soc.* **2011**, *133*, 8775-8777.
(43) Roubelakis, M. M.; Bediako, D. K.; Dogutan, D. K.; Nocera, D. G. *Energy & Environ. Sci.* **2012**, *5*, 7737-7740.
(44) Nakazono, T.; Parent, A. R.; Sakai, K. *Chem. Commun.* **2013**, *49*, 6325-6327.
(45) Wang, D.; Groves, J. T. *Proc. Natl. Acad. Sci. U.S.A.* **2013**, *110*, 15579-15584.
(46) Abe, T.; Nagai, K.; Kabutomori, S.; Kaneko, M.; Tajiri, A.; Norimatsu, T. *Angew. Chem. Int. Ed.* **2006**, *45*, 2778-2781.
(47) Elizarova, G. L.; Matvienko, L. G.; Lozhkina, N. V.; Maizlish, V. E.; Parmon, V. N. *React. Kinet. Catal. Lett.* **1981**, *16*, 285-288.
(48) Tran, P. D.; Goff, A. L.; Heidkamp, J.; Jousselme, B.; Guillet, N.; Palacin, S.; Dau, H.; Fontecave, M.; Artero, V. *Angew. Chem. Int. Ed.* **2011**, *50*, 1371-1374.
(49) Soriano-López, J.; Goberna-Ferrón, S.; Vigara, L.; Carbó, J. J.; Poblet, J. M.; Galán-Mascarós, J. R. *Inorg. Chem.* **2013**, *52*, 4753-4755.
(50) Adler, A. D.; Longo, F. R.; Finarelli, J. D.; Goldmacher, J.; Assour, J.; Korsakoff, L. *J. Org. Chem.* **1967**, *32*, 467.
(51) Han, A.; Wu, H.; Sun, Z.; Jia, H.; Du, P. *Phys. Chem. Chem. Phys.* **2013**, *15*,

12534-12538.
(52) Bezerra, C. W. B.; Zhang, L.; Lee, K.; Liu, H.; Marques, A. L. B.; Marques, E. P.; Wang, H.; Zhang, J. *Electrochim. Acta.* **2008**, *53*, 4937-4951.

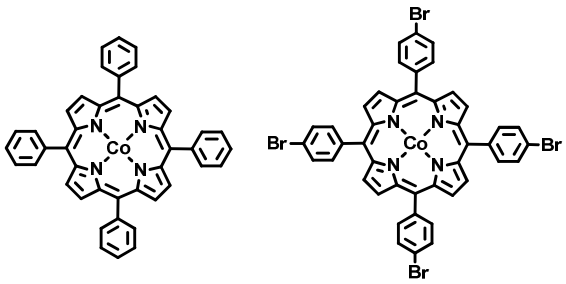

Scheme 1. Molecular structures of **CoP-1** and **CoP-2**.

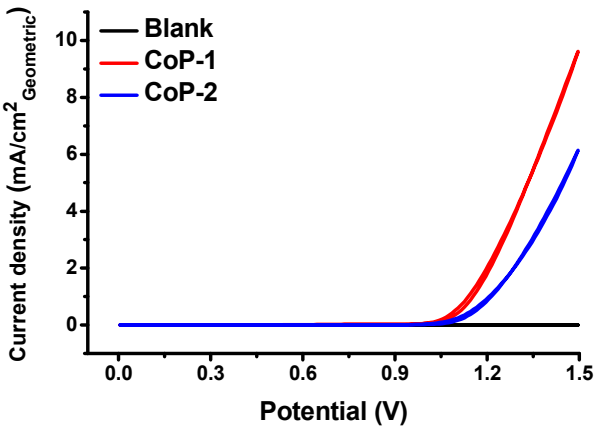

Figure 1. Cyclic voltammograms obtained using FTO coated with 20 nmol/cm^2 cobalt porphyrin complexes as the working electrodes in a 0.5 M Bi solution. Red plot: **CoP-1**, blue plot: **CoP-2**. The black plot was recorded as the control test in the electrolyte solution using bare FTO as the working electrode. The scan rate is 50 mV/s with iR compensation (about 3-8 ohms).

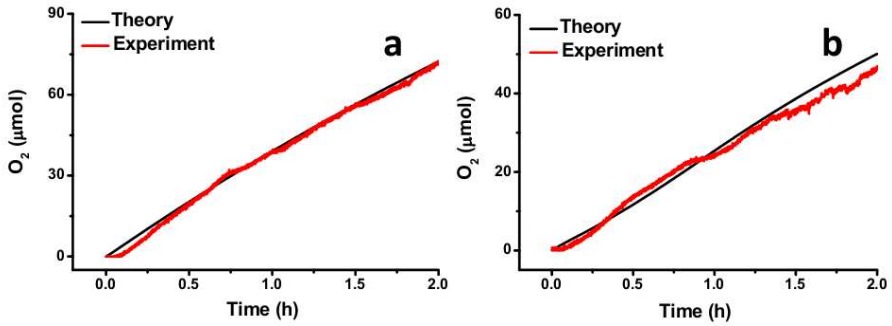

Figure 2. The profiles of oxygen evolution via water oxidation catalyzed by **CoP-1** (a) and **CoP-2** (b). Oxygen gas was detected by fluorescence based oxygen sensor. Black plot: theoretical data; red plot: experimental data.

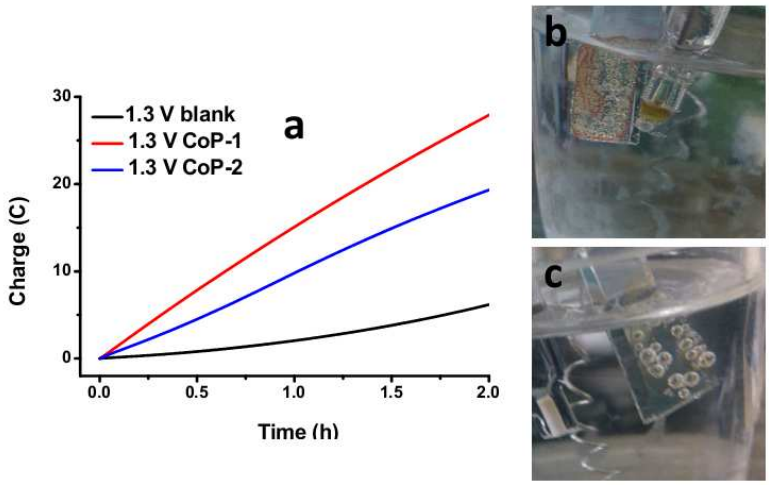

Figure 3. (a) The charge passed through the working electrode during 2-h electrolysis in a 0.5 M Bi solution at 1.3 V, black plot: bare FTO; red plot: **CoP-1**; blue plot: **CoP-2**. (b) Oxygen bubbles formed on the FTO for **CoP-1** during bulk electrolysis; (c) Oxygen bubbles formed on the FTO for **CoP-2** during bulk electrolysis.

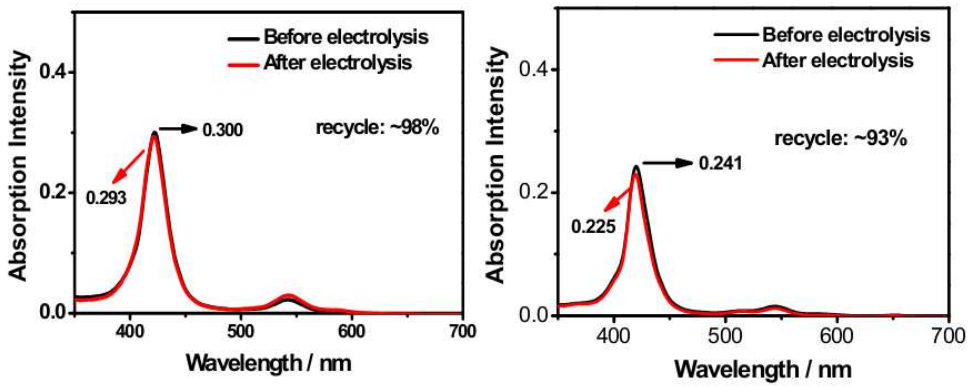

Figure 4. UV-vis spectra of two cobalt porphyrin complexes in THF under the same concentration (1.67×10^{-6} M) (a: **CoP-1**; b: **CoP-2**). Black plot represents the absorption of the freshly prepared cobalt porphyrin complexes in THF and the red plot shows the absorption of the complexes washed from FTO after 10 min of electrolysis.

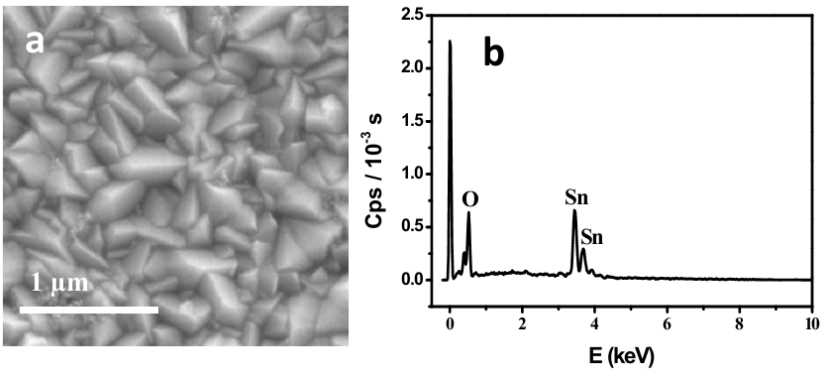

Figure 5. (a) SEM images and (b) EDX data for FTO coated with **CoP-1** after bulk electrolysis and subsequently washed by THF.

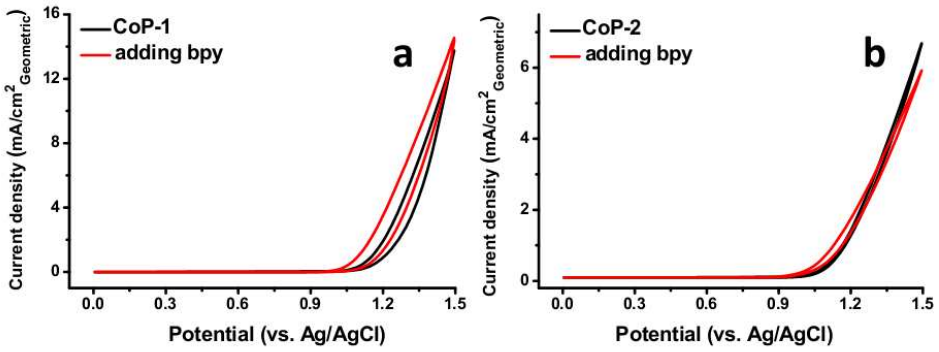

Figure 6. Cyclic voltammograms obtained in a 0.5 M Bi solution by using **CoP-1/CoP-2** coated FTO as the working electrodes. After several CV scans，the electrolyte was added excess of 2,2′-bipyridine (bpy) (80 μmol). Black plot: the CV obtained with no bpy, red plot: the CV obtained with bpy. a: **CoP-1**; b: **CoP-2**. The scan rate is 50 mV/s and there is iR compensation (about 3-8 ohms).

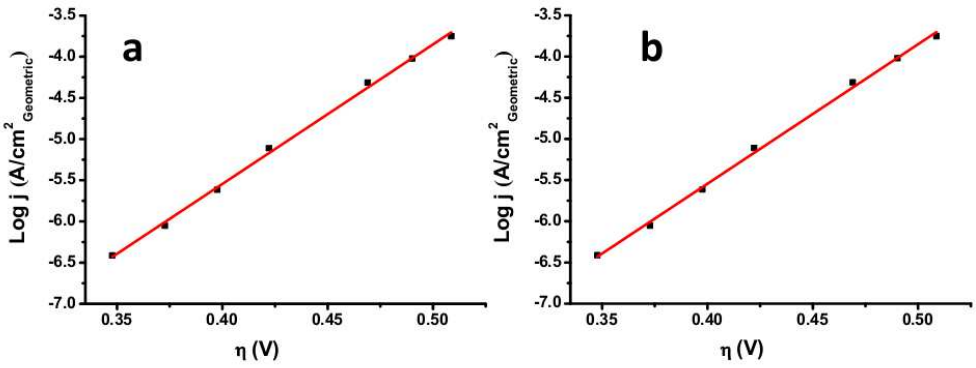

Figure 7. Tafel plot of **CoP-1** and **CoP-2** coated on FTO operated in a 0.1 M Bi at pH 9.2, where η is the overpotential, iR accounts for the uncompensated solution resistance, and E^{θ} is the thermodynamic potential for water oxidation at this pH value. $\eta = E_{applied} - iR - E^{\theta}$. The slopes of the two plots are about ~62 mV/decade and ~59 mV/decade for **CoP-1** (a) and **CoP-2** (b), respectively.

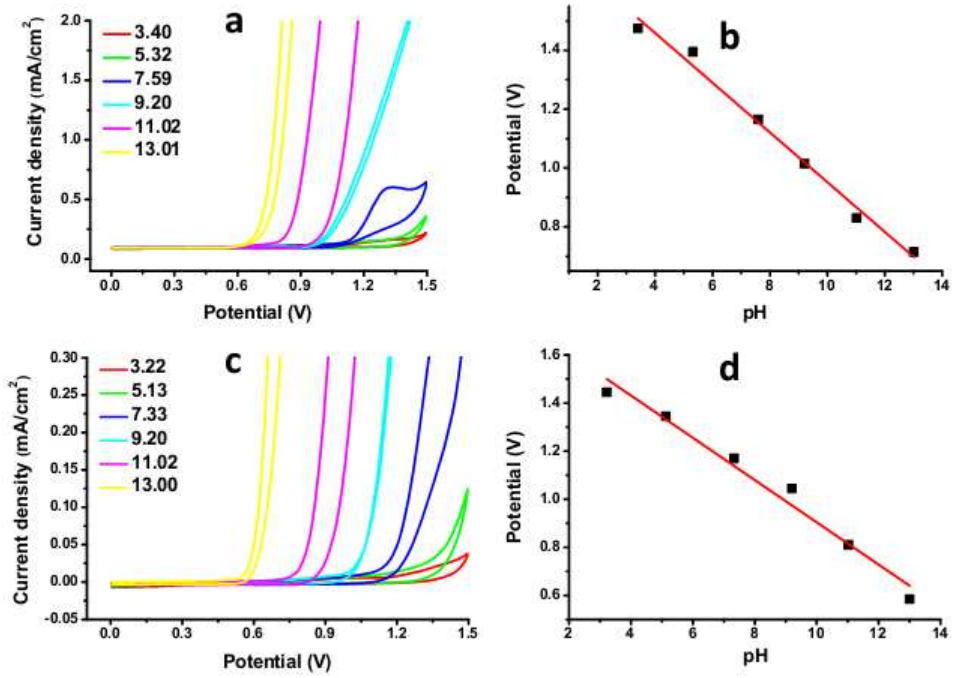

Figure 8. The CVs of the catalysts films coated on FTO at different pH values going from 3.00 to 13.00 for **CoP-1** and **Co-P2** (left, a and c). The plot of the potentials (fixed potential at 200 μA/cm^2 for **CoP-1** and 30 μA/cm^2 for **CoP-2**) versus pH values showed a nearly linear decrease from 3.00 to 13.00 (right, b and d). a-b: **CoP-1**; c-d: **CoP-2**. The CVs were taken at a scan rate of 50 mV/s and the geometric areas of the electrode were used to calculate the current densities.

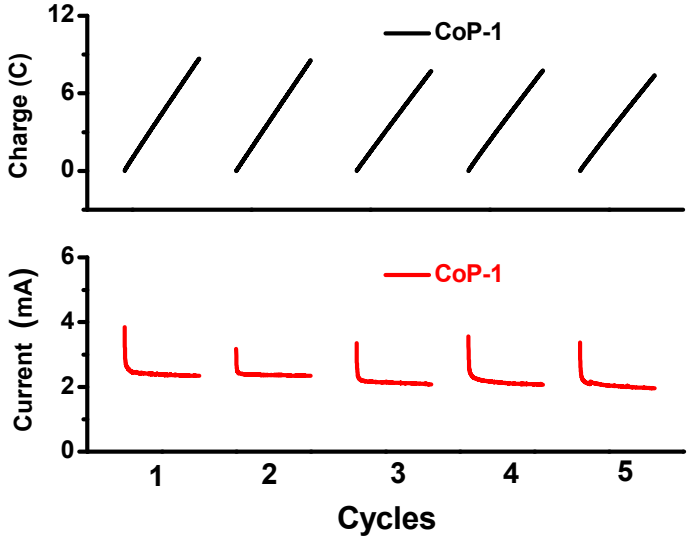

Figure 9. The recyclability of **CoP-1** catalyst film for water oxidation under the controlled potential at 1.3 V in a 0.5 M Bi solution. The black plot represented the passed charge and the red plot displayed the current density during electrolysis. For the whole process, the FTO electrode coated with **CoP-1** film was used, washed with THF after 1 hour electrolysis and reused for another cycle of electrolysis. The electrode area is 1 cm^2.